

Research Article

Study on the Nonlinear Damage Creep Model of the Weak Interlayer

Erjian Wei ^{1,2}, Bin Hu ^{1,2}, Kunyun Tian ³, Peishan Cen,⁴ Zhen Zhang,^{1,2} Zeqi Wang,^{1,2} and Shuxiang Chang^{1,2}

¹School of Resources and Environmental Engineering, Wuhan University of Science and Technology, Wuhan, Hubei, China

²Hubei Key Laboratory for Efficient Utilization and Agglomeration of Metallurgic Mineral Resources, Wuhan, Hubei, China

³School of Resource and Security Engineering, Henan University of Engineering, Zhengzhou, Henan, China

⁴School of Construction Engineering, Zhengzhou Shengda University, Zhengzhou, Henan, China

Correspondence should be addressed to Erjian Wei; weierjian@wust.edu.cn

Received 17 March 2022; Accepted 28 March 2022; Published 8 April 2022

Academic Editor: Xianze Cui

Copyright © 2022 Erjian Wei et al. This is an open access article distributed under the Creative Commons Attribution License, which permits unrestricted use, distribution, and reproduction in any medium, provided the original work is properly cited.

The weak interlayer has become a weak link in slope engineering due to its rheological effect. It is of great significance to study the nonlinear creep model of weak interlayer for long-term stability of the slope. In this paper, based on the creep curve characteristics of weak interlayer and considering the influence of aging damage, the nonlinear improvement of a classical viscoplastic body under stress and time-double threshold conditions is carried out, so that it can more accurately reflect the accelerated creep characteristics of the weak interlayer. By analyzing the relationship between failure load and time, the accelerated creep time threshold of the weak interlayer is obtained. On this basis, a nonlinear damage creep constitutive model of the weak interlayer is constructed and its creep equation is derived. By using the self-defined function fitting tool of Origin software and the Levenberg-Marquardt optimization algorithm, the creep test data of weak interlayer are fitted and compared. The fitting curve is in good agreement with the test data, which shows the rationality and applicability of the nonlinear creep model. The results show that the nonlinear damage creep model constructed in this paper can well describe the creep characteristics of the weak interlayer and the model has important theoretical reference significance for the study of long-term stability of slope with the weak interlayer.

1. Introduction

Rock rheological effect is a common phenomenon in geotechnical engineering. A large amount of slope engineering and tunnel engineering damage is caused by rock rheological effect [1–5]. As a special structural plane, the weak interlayer has low mechanical strength and obvious rheological effect, which often constitutes the weak link in the slope, so it poses a serious threat to the slope stability [6–10]. Therefore, it is necessary to study the rheological mechanical properties of the weak interlayer, and the study of the creep constitutive model of the weak interlayer is the core content [11–15]. Therefore, the study of the creep constitutive model of the weak interlayer has important theoretical significance and practical value for ensuring the long-term stability of slope engineering [16–18].

Generally speaking, there are two methods to establish the rheological constitutive model: the first one is directly fitting the rock rheological test curve with the empirical equation through the rheological test of rock. This method has a good fitting effect, but the physical meaning of the model is not clear. The second is based on the rheological test results, which is composed of series and parallel combinations of traditional model components, and then, the unknown rheological model component parameters are determined by identifying the component model and parameter inversion method [6]. Xia et al. [19] established a unified rheological mechanical model including 15 rheological mechanical properties. Nevertheless, since the traditional rheological model is composed of linear components, no matter how many components are in the

model, the model is more complex. The final model can only reflect the characteristics of linear viscoelastoplasticity and cannot describe the accelerated rheological stage [20]. Therefore, more and more nonlinear rheological models are proposed. Yang et al. [21] proposed a new nonlinear rheological element NRC model by assuming that the nonlinear shear rheological model of rock is a Weibull distribution function of time and combined it with the time function to describe the accelerated rheological stage. Zhao et al. [22] established a new viscoelastic-plastic creep damage model by combining the Burgers model and nonlinear Mohr-Coulomb plastic element in series. Xu et al. [23] defined the piecewise function of the greenschist creep damage variable changing with time by analyzing the whole creep curve of greenschist, proposed the conjecture that creep damage only appeared in the accelerated rheological stage, and established the generalized Bingham model considering the damage variable. Zhang et al. [24] improved the NRC model proposed by Xu et al. combined with the traditional Kelvin model to form a four-element nonlinear viscoelastic-plastic rheological model. Zhu et al. [25] and Huang et al. [26] assumed the creep damage variable of rock as a negative exponential function and used the damage Burgers model to describe the creep characteristics of the rock.

A large number of research results have been achieved in the nonlinear creep model of the rock. However, the research on the creep model of the weak interlayer is relatively rare, and there are few reports on the construction of a nonlinear creep model based on the double thresholds of stress and time. In view of this, based on the series-parallel connection of classical components, this paper introduces the damage variable in the accelerated rheological stage and considers the influence of the time threshold to establish the damage constitutive model that describes the nonlinear rheological properties of the weak interlayer. On this basis, the creep test results of the weak interlayer are nonlinearly fitted to verify the rationality and applicability of the constructed model.

2. Establishment of the Nonlinear Creep Model of the Weak Interlayer

2.1. Creep Curve Characteristics of the Weak Interlayer.

The creep of the weak interlayer is a complex process in which multiple deformations such as elasticity, viscosity, plasticity, viscoelasticity, and viscoplasticity coexist. When the stress of the weak interlayer is less than its long-term strength, the creep curve of the weak interlayer is as shown in Figure 1. The weak interlayer generates elastic strain ε_0 at the moment of loading and then enters the attenuation creep stage. The creep deformation increases continuously, while the creep rate decreases continuously. At time t_a , the creep rate attenuates to zero, and the strain is stable at ε_a . In this case, the classical element combination model can be used to describe the creep characteristics of the rock. When the stress of the weak interlayer exceeds its long-term strength, the creep curve of the weak interlayer is as shown in Figure 2. At the initial stage of loading, the creep characteristics of the

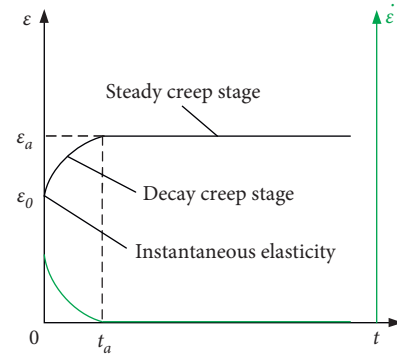


FIGURE 1: Steady-state creep curve.

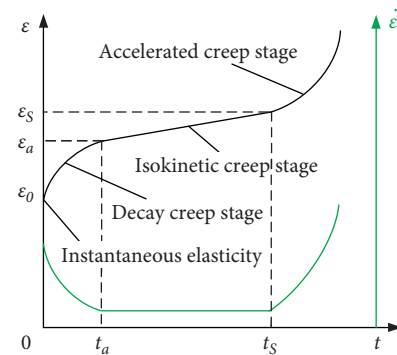


FIGURE 2: Creep failure curve.

weak interlayer are the same as those mentioned above. They all go through the instantaneous elasticity first and then enter the attenuation creep stage. However, starting from the t_a moment, the weak interlayer enters the constant creep stage, the strain of the weak interlayer is still increasing at this stage and the creep rate is a constant value. When the time reaches t_s , the weak interlayer enters the accelerated creep stage and ε_s is the critical strain value of accelerated creep initiation. Since the traditional creep components are linear components, the classical component combination model cannot describe the nonlinear characteristics of accelerated creep. In this paper, the classical components are improved to construct a creep model that can reflect the nonlinear characteristics of the weak interlayer.

2.2. Nonlinear Viscoplastic Body Based on Double Threshold Conditions.

The viscoplastic body composed of classical elements is shown in Figure 3, which is composed of a plastic switch element and a viscous element in parallel. In the figure, τ is the shear stress, η is the viscosity coefficient of the viscous element, and τ_s is the long-term shear strength of the rock. When the stress of the plastic element is not more than τ_s , the plastic element is not opened and the viscoplastic body does not produce strain. When the stress of the plastic element is more than τ_s , the plastic element is opened and the viscoplastic body produces strain. Since the viscous element of the viscoplastic body is a linear element, it cannot describe the nonlinear accelerated creep stage of rock, so it

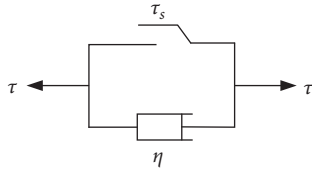


FIGURE 3: Classical viscoplastic body.

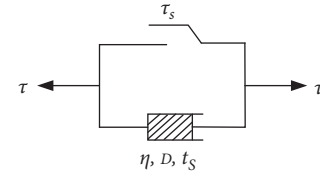


FIGURE 4: Nonlinear viscoplastic body.

needs to be improved. The idea of improvement is to conduct nonlinear treatment of viscous components. A large number of tests show that when the stress of rock is less than its long-term strength, the rock is in the first two stages of creep and no accelerated creep failure occurs. When the stress of the rock exceeds its long-term strength, it is not immediately leading to accelerated creep failure, but at a certain time t_s , the rock enters the accelerated creep stage. According to the current relevant research [6], the aging damage of rock will occur when it enters accelerated creep. Therefore, based on the double threshold conditions of stress and time and considering the influence of aging damage, this paper improves the classical viscoplastic body, and the improved nonlinear viscoplastic body is shown in Figure 4. In the figure, D is the damage variable, t_s is the start time of accelerated creep, and the meaning of other parameters is the same as that of the corresponding parameters in Figure 3.

The damage variable D can be expressed as follows:

$$D = \begin{cases} 0 & t \leq t_s \\ 1 - \frac{1}{a} \exp[-a(t - t_s)] & t > t_s. \end{cases} \quad (1)$$

Here, a is the material parameter, which can be determined by fitting test data; t is the creep time, and t_s is the start time of accelerated creep. The damage variable D value is 0~1. If $t \leq t_s$, then $D=0$; that is, the weak interlayer is not damaged, When t approaches infinity, $D=1$, indicating that the weak interlayer has been destroyed.

Based on the above analysis, we can construct the creep equation of a nonlinear viscoplastic body.

When $\tau \leq \tau_s$, the plastic switch of the nonlinear viscoplastic body is closed and there is no strain in the viscoplastic body; that is, $\varepsilon=0$. When $\tau > \tau_s$ and $t \leq t_s$, the plastic switch of the nonlinear viscoplastic body will be opened, but it has not entered the acceleration stage and the aging damage has not occurred. We regard it as a classical viscoplastic body, so its creep equation can be expressed as follows:

$$\varepsilon = \frac{\tau - \tau_s}{\eta} t. \quad (2)$$

When $\tau > \tau_s$ and $t > t_s$, the plastic switch has been opened and the aging damage has also occurred. The nonlinear viscoplastic body enters the accelerated creep stage. The constitutive equation of the nonlinear viscoplastic body can be expressed as follows:

$$\tau = \tau_s + \eta(1 - D)\dot{\varepsilon} = \tau_s + \eta \frac{1}{a} \exp[-a(t - t_s)]\dot{\varepsilon}. \quad (3)$$

From formula (3),

$$\dot{\varepsilon} = \frac{\tau - \tau_s}{\eta} a \exp[a(t - t_s)]. \quad (4)$$

The creep equation of the nonlinear viscoplastic body is obtained by integrating both sides of (4):

$$\varepsilon = \frac{\tau - \tau_s}{\eta} \exp[a(t - t_s)]. \quad (5)$$

2.3. Determination of Accelerated Creep Time Threshold. From the previous section, we can see that the accelerated creep time threshold t_s reflects the opening time of the accelerated creep of the weak interlayer. It is an important parameter of the creep characteristics of the weak interlayer, which can be determined by the following method.

According to the research of some scholars [27], the failure load of the weak interlayer decreases with the increase in failure time, as shown in Figure 5. τ_0 is the instantaneous strength of the weak interlayer, τ_∞ is the long-term strength of the weak interlayer, and the stress corresponding to the accelerated creep start time t_s is τ . When the stress of the weak interlayer is higher than its long-term strength, the relationship between accelerated creep time threshold and stress can be established from Figure 5, as shown in the following equation:

$$\tau = \exp(-\alpha t_s + \beta). \quad (6)$$

From formula (6),

$$t_s = \frac{\beta - \ln \tau}{\alpha}. \quad (7)$$

Here, α and β are undetermined parameters, which can be determined by fitting test data. The accelerated creep time threshold of the weak interlayer can be determined by formula (7).

2.4. Establishment of the Nonlinear Creep Model. According to the creep characteristics of the weak interlayer, when the stress is less than the stress threshold of accelerated creep, the weak interlayer generates instantaneous elastic strain, decay creep, and steady creep. At this time, the Bergs model can be used to describe the creep characteristics of the weak interlayer. When the stress exceeds the stress threshold of accelerated creep, the rock will eventually enter the nonlinear accelerated creep stage at a certain time point after experiencing the creep deformation of the first two stages. A nonlinear viscoelastic-plastic damage creep model which can describe the whole creep process of the weak interlayer

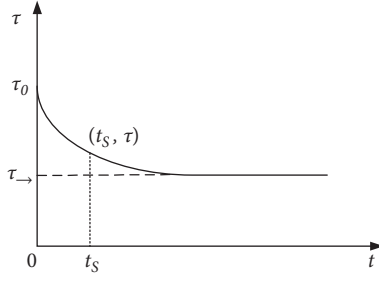


FIGURE 5: Relationship between failure load and time.

can be constructed by using the improved nonlinear viscoplastic body and Bergs body in series. The model is shown in Figure 6. In the figure, I describes the instantaneous elastic strain of the weak interlayer, II reflects the viscoelasticity of the weak interlayer, III reflects the viscosity of the weak interlayer, II and III describe the attenuation creep stage and steady creep stage of the weak interlayer, and IV reflects the nonlinear viscoplasticity of the weak interlayer, which describes the nonlinear accelerated creep stage of the weak interlayer.

It can be seen from Figure 6 that when $\tau \leq \tau_s$, I, II, and III are all involved in creep deformation. The state equations of the creep model are as follows:

$$\begin{cases} \tau = \tau_1 = \tau_2 = \tau_3 \\ \varepsilon = \varepsilon_1 + \varepsilon_2 + \varepsilon_3 \\ \tau_1 = G_1 \varepsilon_1 \\ \tau_2 = \tau_{21} + \tau_{22} = G_2 \varepsilon_2 + \eta_1 \dot{\varepsilon}_2 \\ \tau_3 = \eta_2 \dot{\varepsilon}_3. \end{cases} \quad (8)$$

From formula (8),

$$\varepsilon = \frac{\tau}{G_1} + \frac{\tau}{G_2} \left[1 - \exp\left(-\frac{G_2 t}{\eta_1}\right) \right] + \frac{\tau}{\eta_2} t. \quad (9)$$

When $\tau > \tau_s$, and $t \leq t_s$, I, II, III, and IV all participate in creep deformation; however, the viscoplastic body has not entered the accelerated creep stage, and it has not been damaged. At this time, the state equation of the creep model is as follows:

$$\begin{cases} \tau = \tau_1 = \tau_2 = \tau_3 = \tau_4 \\ \varepsilon = \varepsilon_1 + \varepsilon_2 + \varepsilon_3 + \varepsilon_4 \\ \tau_1 = G_1 \varepsilon_1 \\ \tau_2 = \tau_{21} + \tau_{22} = G_2 \varepsilon_2 + \eta_1 \dot{\varepsilon}_2 \\ \tau_3 = \eta_2 \dot{\varepsilon}_3 \\ \tau_4 = \tau_s + \eta_3 \dot{\varepsilon}_4. \end{cases} \quad (10)$$

From formula (10),

$$\varepsilon = \frac{\tau}{G_1} + \frac{\tau}{G_2} \left[1 - \exp\left(-\frac{G_2 t}{\eta_1}\right) \right] + \frac{\tau}{\eta_2} t + \frac{\tau - \tau_s}{\eta_3} t. \quad (11)$$

When $\tau > \tau_s$, and $t > t_s$, I, II, III, and IV all participate in creep deformation, the viscoplastic body has been damaged, and it has entered the accelerated creep stage. At this time, the state equation of the creep model is as follows:

$$\begin{cases} \tau = \tau_1 = \tau_2 = \tau_3 = \tau_4 \\ \varepsilon = \varepsilon_1 + \varepsilon_2 + \varepsilon_3 + \varepsilon_4 \\ \tau_1 = G_1 \varepsilon_1 \\ \tau_2 = \tau_{21} + \tau_{22} = G_2 \varepsilon_2 + \eta_1 \dot{\varepsilon}_2 \\ \tau_3 = \eta_2 \dot{\varepsilon}_3 \\ \tau_4 = \tau_s + \eta_3 (1 - D) \dot{\varepsilon}_4 = \tau_s + \eta_3 \frac{1}{a} \exp[-a(t - t_s)] \dot{\varepsilon}_4. \end{cases} \quad (12)$$

From formula (12),

$$\varepsilon = \frac{\tau}{G_1} + \frac{\tau}{G_2} \left[1 - \exp\left(-\frac{G_2 t}{\eta_1}\right) \right] + \frac{\tau}{\eta_2} t + \frac{\tau - \tau_s}{\eta_3} \exp[a(t - t_s)]. \quad (13)$$

Therefore, the nonlinear damage creep equation of the weak interlayer is as follows:

$$\begin{cases} \varepsilon = \frac{\tau}{G_1} + \frac{\tau}{G_2} \left[1 - \exp\left(-\frac{G_2 t}{\eta_1}\right) \right] + \frac{\tau}{\eta_2} t & (\tau \leq \tau_s), \\ \varepsilon = \frac{\tau}{G_1} + \frac{\tau}{G_2} \left[1 - \exp\left(-\frac{G_2 t}{\eta_1}\right) \right] + \frac{\tau}{\eta_2} t + \frac{\tau - \tau_s}{\eta_3} t & (\tau < \tau_s, t \leq t_s), \\ \varepsilon = \frac{\tau}{G_1} + \frac{\tau}{G_2} \left[1 - \exp\left(-\frac{G_2 t}{\eta_1}\right) \right] + \frac{\tau}{\eta_2} t + \frac{\tau - \tau_s}{\eta_3} \exp[a(t - t_s)] & (\tau < \tau_s, t > t_s). \end{cases} \quad (14)$$

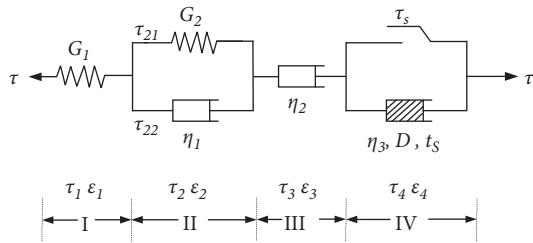


FIGURE 6: Nonlinear damage creep model.

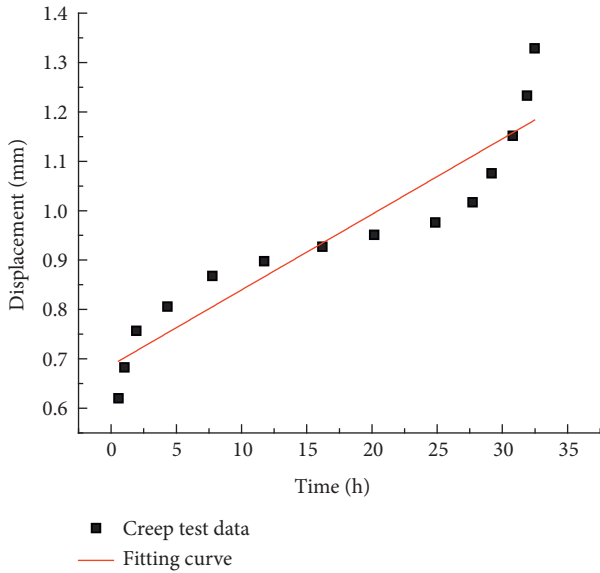


FIGURE 7: Fitting of the integral method.

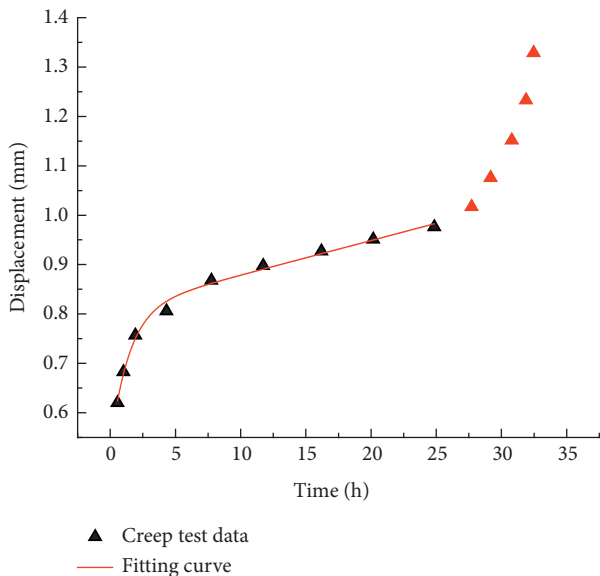


FIGURE 8: Fitting of the first two creep stages.

3. Verification of the Creep Model

By fitting the creep equation derived in the above section to the creep test data of the weak interlayer, the rationality and applicability of the model constructed in this paper can be

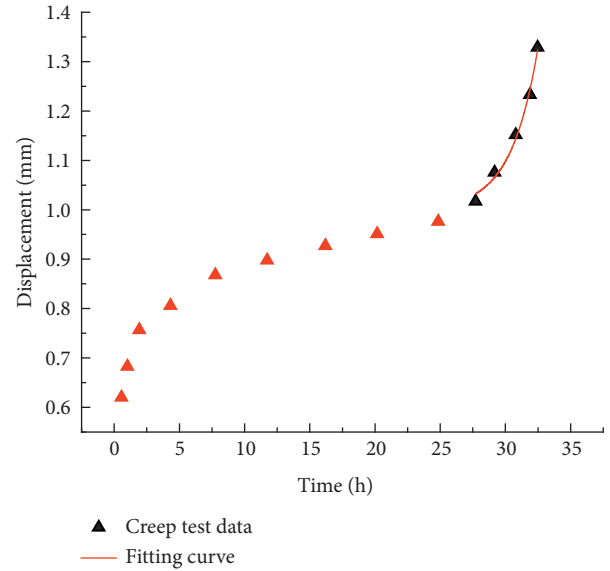


FIGURE 9: Fitting of the accelerated creep stage.

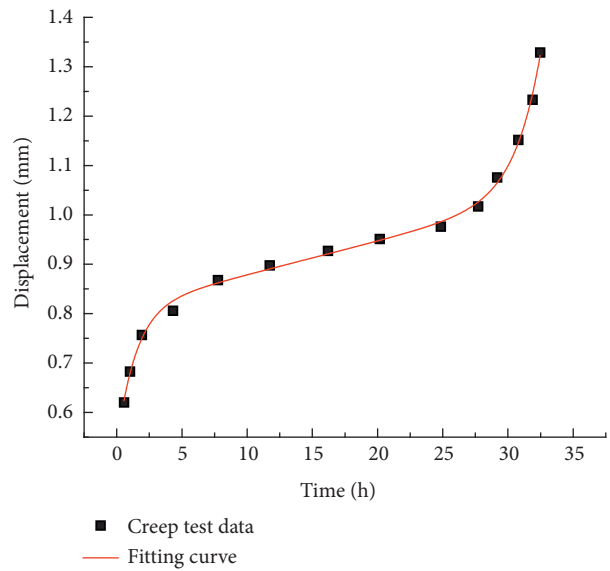


FIGURE 10: Fitting of the improved integral method.

verified. In this paper, data of Zhu et al. [28] were used to conduct shear creep test of the weak interlayer. In the first group of tests, creep tests were carried out on the rock samples with weak interlayers under the normal stress of 0.5 MPa by applying the shear stress step by step. The shear stresses applied at all levels were 0.10 MPa, 0.19 MPa, 0.29 MPa, 0.39 MPa, and 0.59 MPa, respectively. According to the test results, the long-term shear strength of the weak interlayer under this state was 0.423 MPa. In the second group, the creep test was carried out on the rock samples of weak interlayers under a normal stress of 0.7 MPa by applying shear stress in different grades. The applied shear stresses at different levels were 0.216 MPa, 0.432 MPa, 0.648 MPa, 0.864 MPa, 1.080 MPa, and 1.296 MPa, respectively. According to the test results, the long-term shear

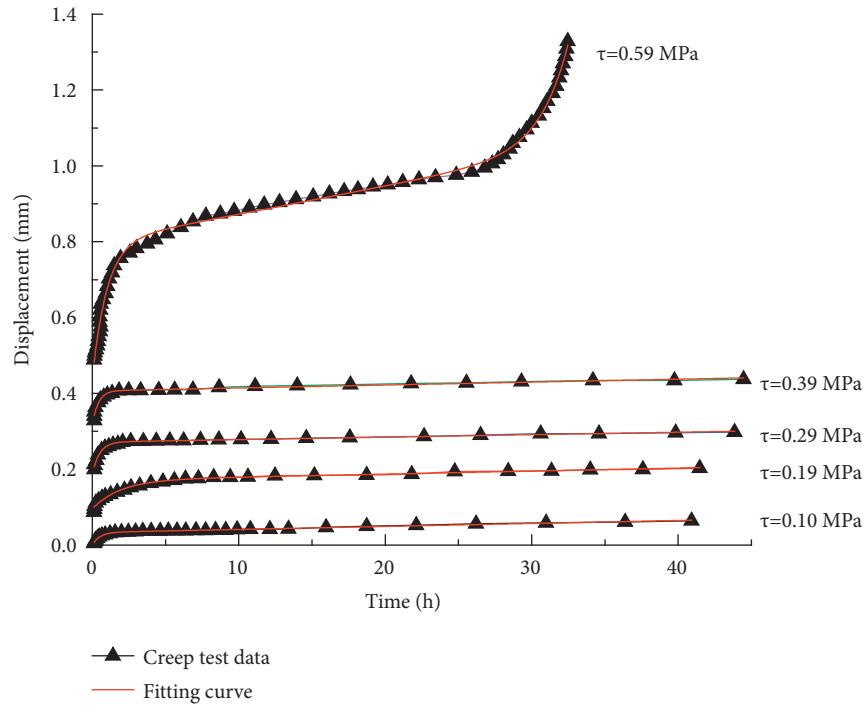


FIGURE 11: Experimental data and the fitting curves ($\sigma = 0.5$ MPa; $\tau = 0.10\sim 0.59$ MPa).

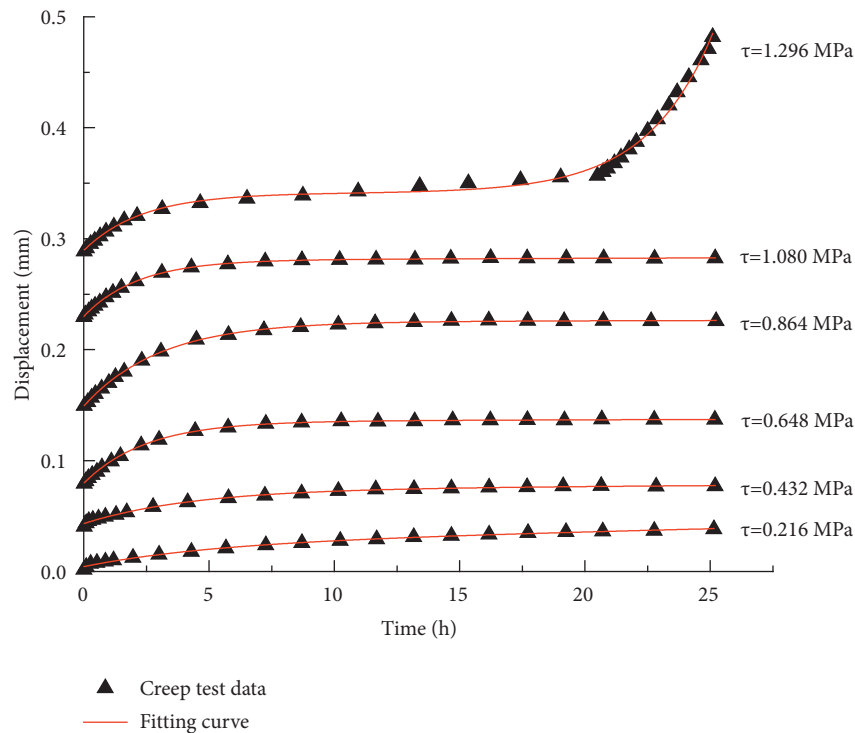


FIGURE 12: Experimental data and the fitting curves ($\sigma = 0.7$ MPa; $\tau = 0.216\sim 1.296$ MPa).

strength of the weak interlayer under this condition was 1.080 MPa. Based on the test results, using the custom function fitting tool of Origin software and Levenberg–Marquardt optimization algorithm, the creep test data of weak interlayers under different shear stresses are fitted and analyzed.

It should be pointed out that for the three stages of complete creep, because the creep equation is more complex, the creep parameters are more and the initial value of the parameters to be optimized is difficult to determine; if the whole method is used for fitting, the results will be as shown in Figure 7, indicating that the fitting has failed. Therefore,

TABLE 1: Creep parameter identification results ($\sigma = 0.5$ MPa; $\tau = 0.10\sim 0.59$ MPa).

τ /MPa	G1/MPa	G2/MPa	η_1 /MPa-mm-1 h	η_2 /MPa-mm-1 h	η_3 /MPa-mm-1 h	a	R2
0.1	3.01	2.98	1.53	127.34			0.9937
0.19	1.99	2.49	4.77	239.54			0.9851
0.29	1.55	3.38	1.64	446.51			0.9893
0.39	1.24	4.21	1.66	505.75			0.9758
0.59	1.34	1.64	1.65	79.41	5.61	0.51	0.9963

TABLE 2: Creep parameter identification results ($\sigma = 0.7$ MPa; $\tau = 0.216\sim 1.296$ MPa).

τ /MPa	G1/MPa	G2/MPa	η_1 /MPa-mm-1 h	η_2 /MPa-mm-1 h	η_3 /MPa-mm-1 h	a	R2
0.216	49.11	10.34	53.49	402.27			0.9942
0.432	10.01	13.91	61.04	3256.51			0.9954
0.648	8.15	11.61	28.67	9076.81			0.9968
0.864	5.79	11.34	34.44	21063.37			0.9989
1.080	4.69	21.21	45.61	14321.18			0.9983
1.296	4.47	25.05	58.41	3.93	8.78	0.38	0.9931

the fitting method needs to be improved. Firstly, the complete creep curve is divided into two parts, which are the first two stages of the creep curve and the accelerated creep curve. They are fitted, respectively, and the initial values of each creep parameter are obtained, as shown in Figure 8 and Figure 9. Secondly, by using these initial creep parameters and using the integral method to fit the complete creep curve, the ideal fitting effect can be obtained, as shown in Figure 10.

This method is used to fit the creep test data of these two groups of weak interlayers. The fitting curves are shown in Figures 11 and 12. The creep model parameters are obtained by fitting, as shown in Tables 1 and 2.

From Figures 11 and 12, it can be seen that the creep test data of weak interlayers under various loads are in good agreement with their fitting curves and the correlation coefficients in Tables 1 and 2 are basically above 0.95, which indicates that the nonlinear damage creep model constructed in this paper can well describe the instantaneous deformation, attenuation creep stage, steady creep stage, and accelerated creep stage of the weak interlayer, which further illustrates the rationality and applicability of the model.

4. Conclusions

- (1) Based on the double threshold conditions of stress and time and considering the influence of aging damage, the classical viscoplastic body is improved in this paper. The improved nonlinear viscoplastic body can more accurately reflect the characteristics of the accelerated creep stage.
- (2) In the fitting analysis of creep curves containing complete three stages, the effect of the complete method is usually poor. In this paper, a piecewise fitting method with a good fitting effect is innovatively proposed.
- (3) The creep test data of weak interlayers are fitted and analyzed by the creep model constructed in this paper. The results show that the fitting curve is in good agreement with the experimental data,

indicating that the nonlinear damage creep model constructed in this paper can well describe the creep characteristics of the weak interlayer. This model can provide important theoretical support for the study of long-term stability of slopes with weak interlayers.

Data Availability

The data used to support the findings of this study are included within the article.

Conflicts of Interest

The authors declare that they have no conflicts of interest.

Acknowledgments

This work was financially supported by the National Natural Science Foundation of China under Grants U1802243 and 41672317, in part by the Hubei Province Technical Innovation Special (major projects) Project under Grant 2017ACA184, in part by the Major Science and Technology Projects of WUST Cultivate Innovation Teams under Grant 2018TDX01, in part by the Program for Innovative Research Team (in Science and Technology) in University of Henan Province under Grant 22IRTSTHN009, and in part by the Science and Technology Project of Henan Province for Tackling Key Problems under Grant 222102320466.

References

- [1] B. Bai, Q. Nie, Y. Zhang, X. Wang, and W. Hu, "Cotransport of heavy metals and SiO₂ particles at different temperatures by seepage," *Journal of Hydrology*, vol. 597, Article ID 125771, 2021.
- [2] H. Tang, D. P. Wang, and Z. Duan, "New maxwell creep model based on fractional and elastic-plastic elements," *Advances in Civil Engineering*, vol. 2020, Article ID 9170706, 11 pages, 2020.
- [3] G. Peng, Z. Q. Chen, and J. R. Chen, "Research on rock creep characteristics based on the fractional calculus meshless

- method," *Advances in Civil Engineering*, vol. 2018, Article ID 1472840, 6 pages, 2018.
- [4] B. Hu, P.-Z. Pan, W.-W. Ji, S. Miao, D. Zhao, and T. Yao, "Study on probabilistic damage constitutive relation of rocks based on maximum-entropy theory," *International Journal of Green Nanotechnology*, vol. 20, no. 2, pp. 1–10, Article ID 06019018, 2020.
- [5] S.-Q. Yang, P. Xu, Y.-B. Li, and Y.-H. Huang, "Experimental investigation on triaxial mechanical and permeability behavior of sandstone after exposure to different high temperature treatments," *Geothermics*, vol. 69, pp. 93–109, 2017.
- [6] J. Sun, "Rock rheological mechanics and its advance in engineering applications," *Chinese Journal of Rock Mechanics and Engineering*, vol. 26, pp. 1081–1106, 2007.
- [7] H. Lin, X. Zhang, Y. X. Wang et al., "Improved nonlinear nishihara shear creep model with variable parameters for rock-like materials," *Advances in Civil Engineering*, vol. 2020, Article ID 7302141, 15 pages, 2020.
- [8] Q. Zhang, Z. P. Song, J. B. Wang, Y. W. Zhang, and T. Wang, "Creep properties and constitutive model of salt rock," *Advances in Civil Engineering*, vol. 2021, Article ID 8867673, 29 pages, 2021.
- [9] R.-l. Shan, Y. Bai, Y. Ju, T.-y. Han, H.-y. Dou, and Z.-l. Li, "Study on the triaxial unloading creep mechanical properties and damage constitutive model of red sandstone containing a single ice-filled flaw," *Rock Mechanics and Rock Engineering*, vol. 54, no. 2, pp. 833–855, 2021.
- [10] B. Bai, R. Zhou, G. Cai, W. Hu, and G. Yang, "Coupled thermo-hydro-mechanical mechanism in view of the soil particle rearrangement of granular thermodynamics," *Computers and Geotechnics*, vol. 137, Article ID 104272, 2021.
- [11] H. Li, N. T. William, J. Daemen, J. Zhou, and C.-k. Ma, "A power function model for simulating creep mechanical properties of salt rock," *Journal of Central South University*, vol. 27, no. 2, pp. 578–591, 2020.
- [12] L. Yang and Z.-d. Li, "Nonlinear variation parameters creep model of rock and parametric inversion," *Geotechnical & Geological Engineering*, vol. 36, no. 5, pp. 2985–2993, 2018.
- [13] Z.-y. Wang, J. Xu, Y.-p. Li, and Y. Wang, "Rheological damage FEA of hydro-mechanical coupling for rock mass," *Journal of Central South University of Technology*, vol. 14, no. S1, pp. 324–328, 2007.
- [14] B. Hu, E. J. Wei, J. Li, X. Zhu, K. Y. Tian, and K. Cui, "Nonlinear creep model based on shear creep test of granite," *Geomechanics and Engineering*, vol. 27, no. 5, pp. 527–535, 2021.
- [15] Y. Zhao, Y. Wang, W. Wang, W. Wan, and J. Tang, "Modeling of non-linear rheological behavior of hard rock using triaxial rheological experiment," *International Journal of Rock Mechanics and Mining Sciences*, vol. 93, pp. 66–75, 2017.
- [16] R. Hou, K. Zhang, J. Tao, X. Xue, and Y. Chen, "A nonlinear creep damage coupled model for rock considering the effect of initial damage," *Rock Mechanics and Rock Engineering*, vol. 52, no. 5, pp. 1275–1285, 2019.
- [17] P. Cao, Y. D. Wen, Y. X. Wang, H. P. Yuan, and B. X. Yuan, "Study on nonlinear damage creep constitutive model for high-stress soft rock," *Environmental Earth Sciences*, vol. 75, pp. 1–8, 2016.
- [18] E. J. Wei, B. Hu, J. Li et al., "Nonlinear viscoelastic-plastic creep model of rock based on fractional calculus," *Advances in Civil Engineering*, vol. 2022, Article ID 3063972, 7 pages, 2022.
- [19] C. C. Xia, X. D. Wang, C. B. Xu, and C. S. Zhang, "Method to identify rheological model by unified rheological model theory and case study," *Chinese Journal of Rock Mechanics and Engineering*, vol. 27, pp. 1594–1600, 2008.
- [20] B.-R. Chen, X.-J. Zhao, X.-T. Feng, H.-B. Zhao, and S.-Y. Wang, "Time-dependent damage constitutive model for the marble in the Jinping II hydropower station in China," *Bulletin of Engineering Geology and the Environment*, vol. 73, no. 2, pp. 499–515, 2014.
- [21] S. Q. Yang, W. Y. Xu, and S. L. Yang, "Investigation on shear rheological mechanical properties of shale in Longtan Hydropower Project," *Rock and Soil Mechanics*, vol. 28, no. 5, pp. 895–902, 2007.
- [22] Y. L. Zhao, J. Z. Tang, and C. C. Fu, "Rheological test of separation between viscoelastic-plastic strains and creep damage model," *Chinese Journal of Rock Mechanics and Engineering*, vol. 35, no. 7, pp. 1297–1308, 2016.
- [23] W. Y. Xu, S. Q. Yang, and W. J. Chu, "Nonlinear viscoelastoplastic rheological model (hohai model) of rock and its engineering application," *Chinese Journal of Rock Mechanics and Engineering*, vol. 25, no. 3, pp. 433–447, 2006.
- [24] Z. L. Zhang, W. Y. Xu, and W. Wang, "Study of triaxial creep tests and its nonlinear visco-elastoplastic creep model of rock from compressive zone of dam foundation in Xiangjiaba hydropower station," *Chinese Journal of Rock Mechanics and Engineering*, vol. 30, no. 1, pp. 132–140, 2011.
- [25] J. B. Zhu, B. Wang, and A. Q. Wu, "Study of unloading triaxial rheological tests and its nonlinear damage constitutive model of Jinping hydropower station green sandstone," *Chinese Journal of Rock Mechanics and Engineering*, vol. 29, no. 3, pp. 528–534, 2010.
- [26] Y. Y. Huang and H. Zheng, "Preliminary study of equivalent damage rheological model for jointed rock," *Rock and Soil Mechanics*, vol. 32, pp. 3566–3570, 2011.
- [27] L. Q. Li, W. Y. Xu, and W. Wang, "A nonlinear viscoelastoplastic rheological model based on Nishihara's model," *Chinese Journal of Theoretical and Applied Mechanics*, vol. 41, no. 5, pp. 671–680, 2009.
- [28] S. N. Zhu, Y. P. Yin, and B. Li, "Shear creep behavior of soft interlayer in Permian carbonaceous shale," *Rock and Soil Mechanics*, vol. 40, no. 4, pp. 1377–1386, 2019.